

## Dissolved gas dynamics in perennially ice-covered Lake Fryxell, Antarctica

E. M. Hood, B. L. Howes, and W. J. Jenkins

Woods Hole Oceanographic Institution, Clark 459, Woods Hole, Massachusetts 02543

### Abstract

We use the concentrations of noble gases (He, Ne, and Ar), helium isotopes, and tritium to characterize the mechanisms and rates of ventilation for Lake Fryxell, Antarctica, as well as the physical processes controlling dissolved gases. The upper oxic zone is ventilated on timescales of several decades. The anoxic bottom waters are weakly ventilated, with a turnover time of ~3,800 years. In the upper euphotic zone, helium and neon are greatly undersaturated with respect to solubility equilibrium with the atmosphere, whereas argon is greatly supersaturated owing to equilibrium partitioning of the gases between ice, water, and air inclusions in the ice. In the bottom waters, the inert dissolved gas concentrations may be remnants of a near-desiccation event that occurred ~2,000 years B.P., consistent with current paleoclimatic theories.

Lake Fryxell is a perennially ice-covered lake in the Dry Valley Region of southern Victoria Land, Antarctica. It is ~5 km long, 1.6 km wide, and has a maximum depth of 18 m. It is fed by glacial meltstreams from nearby Canada and Commonwealth glaciers, which discharge  $1.6 \times 10^9$  liters  $\text{yr}^{-1}$  into the lake, and has a volume of  $\sim 4.32 \times 10^{10}$  liters (Green et al. 1988). The ice cover has an average thickness of ~5 m. Liquid lakes exist in this desert region of Antarctica because thick ice covers effectively insulate the water below from annual mean air temperatures of  $-20^\circ\text{C}$ . The edge of the ice cover melts during the brief Antarctic summer, creating a moat a few meters wide through which sediments and meltwater enter the lake. Water is removed from the lake through ice formation at the base of the ice cover, ablation and sublimation from the ice surface, and, to a lesser extent, evaporation at the moat. The ice cover greatly restricts wind-generated mixing, as well as gas exchange with the atmosphere, and along with a salinity gradient that extends throughout the water column, creates a highly stable, amictic water column that is anoxic below ~10 m (Fig. 1).

Large supersaturations of several dissolved inert gases are observed at the ice–water interface of these lakes, owing to the exclusion of the gases from the ice lattice as water freezes at the bottom of the ice cover (Burton 1981; Bari and Hallett 1974). As the dissolved gas concentrations in the water reach a critical supersaturation, bubbles form and become incorporated into the growing ice cover, and are eventually removed by ablation of the ice at the surface (Bari and Hallett 1974; Carte 1961). This is a major removal mechanism for gases from the lake.

The hydrological balances of these lakes are thought to be sensitive indicators of climate change on decadal timescales (Chinn 1993; Wharton et al. 1989), and because of the low vertical mixing rates and limited terrestrial inputs,

the lakes provide model environments in which to study the biogeochemical cycles of carbon, methane, and sulfur in aquatic systems (Smith et al. 1993). However, the physical limnology of the lake, which impinges on the hydrological balances as well as the biogeochemical cycles, is not well understood. In this study we use the noble gases (He, Ne, Ar), helium isotopes, and tritium to examine the ventilation mechanisms and rates of Lake Fryxell and the physical processes affecting the dissolved gas cycles.

### Methods

We measured the concentrations of He, Ne, and Ar throughout the water column at 1-m intervals at a station located over the deepest part of the lake basin. Multiple samples from each depth were collected from the center of the lake during the 1993–1994 austral summer. Depths are referenced from the piezometric surface (i.e. the surface of the water in the drill hole). The ice–water interface is located at ~4.7 m. Water samples for the He isotopes and Ne analyses were collected from Kemmerer bottles and stored in crimped copper tubes (Weiss 1969). Tritium samples were collected in 1-liter, treated Flint glass bottles fitted with high-density polyethylene caps. Argon was analyzed on site by gas chromatography. Helium isotopes and concentrations were measured on a statically operated, magnetic sector, dual-collecting mass spectrometer, and the Ne was measured by peak-height manometry using a quadrupole mass spectrometer (Lott and Jenkins 1984). Tritium was measured by the  $^3\text{He}$  in-growth technique (Clarke et al. 1976; Jenkins et al. 1983). Measurement uncertainties are  $\pm 0.25\%$  for He,  $\pm 1\%$  for Ne, and  $\pm 0.01$  tritium unit (T.U.,  $^3\text{H}/\text{H} \times 10^{18}$ ) for tritium.

### Results

*Dissolved gases in the upper oxic waters*—Near the ice–water interface, Ar is supersaturated with respect to solubility equilibrium with the atmosphere, similar to supersaturations of gases reported for other Antarctic lakes (Craig et al. 1992; Wharton et al. 1993), whereas He and Ne are substantially undersaturated (Fig. 2A,B). We suggest that the latter is the result of the large partitioning of the sparingly

### Acknowledgments

We thank Dale Goeringher and L. D. Schlezinger for assistance in the field, Dempsey Lott for his invaluable assistance in the laboratory, and Peter Schlosser, Mark Kurz, Craig Taylor, Tom Torgersen, Mark Altabet, and two anonymous reviewers for helpful comments.

Financial support was provided by the National Science Foundation grants DPP 91-18363 and OCE 93-02812.

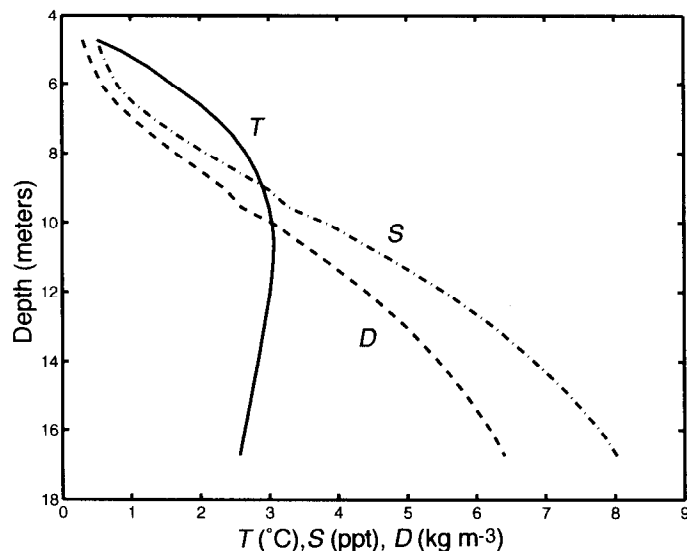


Fig. 1. Profiles of temperature (°C, —), salinity (ppt, ---), and  $\sigma\theta$  (kg m<sup>-3</sup>, -.-).

soluble gases He and Ne between bubbles at the ice–water interface, coupled with the solubility of these gases within the ice itself (Kahane et al. 1969; Namoiit and Bukhgalter 1965). In a relatively closed, three-phase system consisting of ice, air bubbles in the ice, and water, the water will become undersaturated in He and Ne with respect to solubility equilibrium with the atmosphere if it is not adequately ventilated. We propose that this is the case for He and Ne at the ice–water interface of Lake Fryxell.

Craig et al. (1992) measured the gas content of air bubbles within the ice cover of neighboring Lake Hoare, and they presented a model calculation for the two-phase gas distribution for the gases at the ice–water interface. We extend the two-phase equilibrium-partitioning model to include a third phase of solution in ice for He and Ne, using the basic mass-balance equation

$$C_{in}M_{in} = C_{rw}M_{rw} + C_iM_i + C_bV_b \quad (1)$$

where  $M$  is the mass or volume of the reservoir and  $C$  is the concentration of the dissolved gas in the input water ( $C_{in}$ ), the remaining input water ( $C_{rw}$ ), the ice ( $C_i$ ), and the air bubble ( $C_b$ ).  $C_{in}$  is taken to be the equilibrium solubility of the gas with the atmosphere at 0°C.

The input volume of water to the lake via meltstreams varies considerably from year to year (Lawrence and Hendy 1985). We thus present the masses and volumes of the system in relative terms that allow for calculations to be made without determining specific volumes or masses. Approximately 80% of the incoming meltwater is frozen at the ice–water interface (Craig et al. 1992). We used a volume of bubbles in the ice equal to 14.2 cm<sup>3</sup> kg<sup>-1</sup> of original input water, estimated using a gas partitioning of 20.6 cm<sup>3</sup> (STP) kg<sup>-1</sup> of original input water (Craig et al. 1992) and corrected for an ambient pressure at the ice–water interface of 1.45 atm. The concentrations of the gases in each of the reservoirs are related by their equilibrium partition coefficients between the water, ice, and air bubbles in the ice (Table 1).

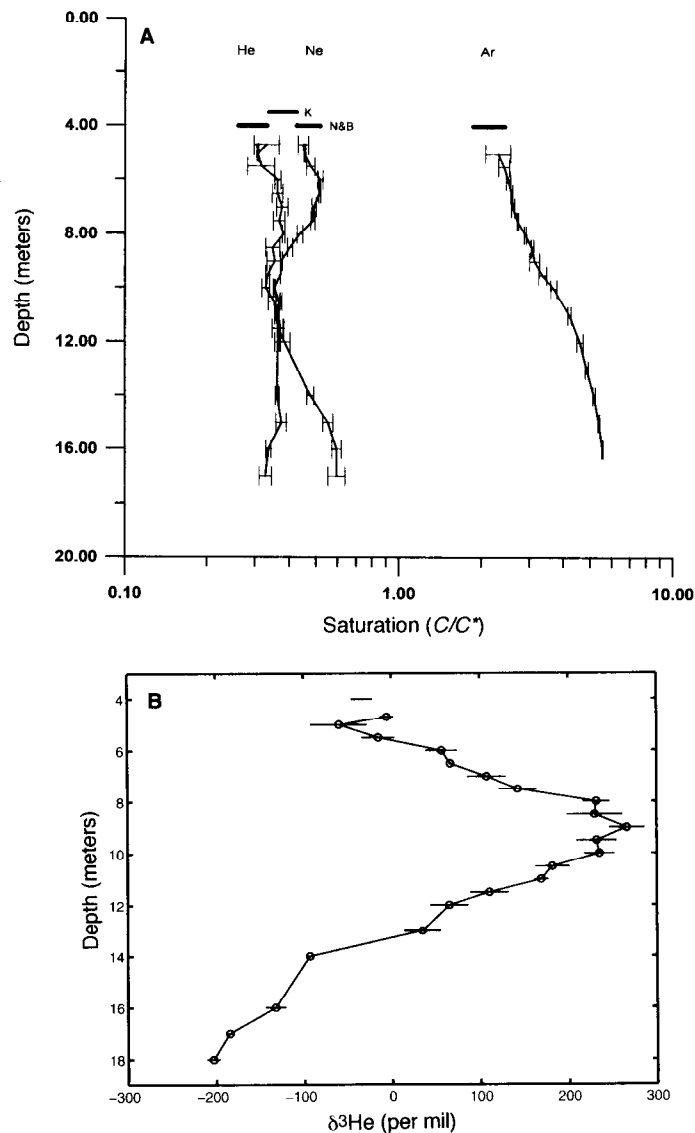


Fig. 2. A. Profiles of He, Ne, and Ar given as saturation with respect to solubility equilibrium (i.e. equilibrium = 1). Depth is referenced from the piezometric surface of the water. Saturations predicted by the three-phase equilibrium-distribution model at the ice–water interface are shown as bars at the top of each profile. For He and Ne, predictions using the solubility values of Namoiit and Bukhgalter (1965) are shown. The uncertainties of the concentrations are calculated from the standard deviations of replicate samples for each depth. The partition coefficients were taken from the Bunsen solubility values reported by Weiss (1970, 1971). B.  $\delta^3\text{He}$  profile:  $\delta^3\text{He} = [(R_s/R_a) - 1]1,000$ , where  $R_s$  is the  $^3\text{He}/^4\text{He}$  sample and  $R_a$  is  $^3\text{He}/^4\text{He}$  atmosphere. The model prediction of  $\delta^3\text{He}$  at the ice–water interface is shown as a thick horizontal bar. The helium isotope data are taken from Benson and Krause (1980).

To our knowledge, two sets of values for the solubility of He and Ne in ice are available. While the values of the solubility of He in ice that are reported in these two references are in good agreement, the values for the solubility of Ne in ice disagree. Kahane et al. (1969) reported that, like He, the ratio of the solubility of Ne in ice to that in water

Table 1. Equilibrium partition coefficients for He, Ne, and Ar in a three-phase system. Partition coefficients were calculated using the Bunsen solubility coefficients of Weiss (1970, 1971).

Partition	Ar	Ne*	Ne†	He
Bubble/water	18.65	81.02	81.02	106.8
Bubble/ice	∞	56.25	90.02	56.89
Ice/water	0	1.4	0.9	1.9

\* Calculated using the solubility values of Ne in ice from Kahane et al. (1969).

† Calculated using the solubility values of Ne in ice from Namoit and Bukhgalter (1965).

is  $>1$ , whereas Namoit and Bukhgalter (1965) stated that the ratio is slightly  $<1$ . However, in this system, both sets of values predict the observations at the ice–water interface within the uncertainties of the mass balance calculation. We use both sets of solubility values throughout the work.

The partitioning of the gases between the three phases and the relationship of the reservoirs as described by the mass balance equation provide a system of three equations that are solved to obtain the concentrations of the gases in each of the reservoirs. The dissolved gas concentrations at the ice–water interface predicted by this model for He, Ne, Ar, (Fig. 2A), and  $\delta^3\text{He}$  (Fig. 2B) are in good agreement with the observed concentrations.

Table 2 contains model estimates of the gas saturations without dissolution in ice (removal by bubbles only) and without bubble formation (gas saturations prior to bubble formation), as well as a comparison of these estimates using different values of He and Ne solubility in ice. The saturations of He and Ne are consistent with a three-phase equilibrium balance, whereas the two-phase systems substantially overpredict the saturations. We stress that this equilibrium-partitioning process must be viewed as an annual net effect. During initial ice formation, the gas saturations result from partitioning between ice and water. Upon nucleation of bubbles at the ice–water interface, the gases are further partitioned into the bubble phase. However, the

Table 2. Comparison of observed gas saturations and model calculations. Saturations are reported as the ratio of the measured concentrations to the concentration at solubility equilibrium with the atmosphere. ("Observed" indicates the observed saturations at the ice–water interface; 3-phase, the predicted three-phase system saturations using the solubility values of Ne in ice; 2-phase (in column 4), the predictions for two-phase (bubble–water) case with no solubility of gases in ice; and 2-phase (in columns 5 and 6) shows the predicted saturations for freezing with no bubble formation.)

	Observed	3-phase*	3-phase†	2-phase	2-phase*	2-phase†
He	0.33±0.04	0.30±0.04	0.29±0.04	0.63	0.54	0.51
Ne	0.45±0.02	0.38±0.05	0.47±0.05	0.74	0.68	1.01
Ar	2.31±0.005	2.15±0.28	2.15±0.28	2.15	5.0	5.0
Ne/He	1.36±0.22	1.27±0.31	1.62±0.16			

\* Calculated using the solubility values of Ne in ice from Kahane et al. (1969).

† Calculated using the solubility values of Ne in ice from Namoit and Bukhgalter (1965).

strong, stable stratification of the lake and the tritium- $^3\text{He}$  age profile (Fig. 3A, *see below*) suggest little vertical mixing. The saturations generated at any stage of the annual freezing process are therefore unlikely to be mixed significantly below the interface, and the molecular diffusive timescales of the gases are not sufficient to transport the gases more than a fraction of a meter over the course of a year. We interpret the net annual partitioning of gases near the ice–water interface as an essentially closed system in which the initial meltwater input remains very near the interface throughout the freezing cycle. Additionally, because the partitioning of the gases into the bubble phase is dominant, the discrepancy between the low solubility values for Ne in the ice phase becomes indistinguishable within the uncertainties of the mass balance calculation.

We suggest that small variations in saturations seen in the profiles in the upper waters below the ice–water interface may result from changes in the meltwater input volume, freezing, the bubble volume in the ice, or melting of the ice at the interface. For instance, increases in Ne and He seen between 6 and 8 m may be caused by melting of the ice cover or by a period of decreased freezing relative to meltwater input. Tritium- $^3\text{He}$  ages show the 6–8-m water to be  $\sim 10$  years old. Chinn (1993) reported that the ice cover of Lake Fryxell thinned  $\sim 2$  m over a period  $\sim 10$  years ago. However, the quality of the data presented here is not sufficient to discriminate between these processes, and both long- and short-term variability in the hydrological parameters of the lake can easily generate saturation changes of the sizes observed. Given the data and the constraints on the hydrological system at hand, we can only suggest that the general mechanism that controls the saturations of the inert gases at the ice–water interface seems to be partitioning of gases between the water, air bubbles in the ice, and, for He and Ne, the ice matrix itself.

*Dissolved gases in the anoxic bottom waters*—We focus first on the concentrations of Ar and Ne, and then discuss the He concentrations, which respond to additional processes in the bottom waters. The Ar concentrations increase to  $\sim 5.75$  times greater than solubility equilibrium, whereas the Ne concentrations decrease further to 0.33 times the solubility equilibrium. We calculate that the production of  $^{40}\text{Ar}$  by the decay of  $^{40}\text{K}$  in 230 m of sediment below the lake is  $\sim 1 \times 10^7$  atoms  $\text{m}^{-2} \text{s}^{-1}$ . The observed gradient of Ar in the bottom water implies a minimum upward flux (assuming the vertical mixing to be no greater than molecular diffusion) of  $\sim 7 \times 10^{12}$  atoms  $\text{m}^{-2} \text{s}^{-1}$ , which is 5–6 orders of magnitude larger than can be supported by  $^{40}\text{K}$  decay from the sediments.

The deep supersaturation of Ar could result from bottom water that was created in the past by slightly different freezing processes at the ice–water interface. We describe below one possible scenario for an alternative freezing processes at the interface, and constrain and support this scenario by using the concentrations of the dissolved gases and the balance between the hydrostatic pressure and total dissolved gas pressure (the latter determines whether and to what extent bubble formation will occur). The presence or absence of bubble formation in the ice is of paramount importance in

Table 3. Concentrations of the major dissolved gases in the surface and bottom waters. Concentrations are given in cc (STP) g<sup>-1</sup>; saturations are calculated as  $C/C^*$ , where  $C$  is the concentration of the gas in the water and  $C^*$  is the concentration at solubility equilibrium with the atmosphere.

	Nitrogen	Oxygen	Argon	Argon/N <sub>2</sub>	Neon
Surface	0.015±0.004	0.029±0.002	1.2×10 <sup>-3</sup> ±1×10 <sup>-4</sup>		1.04×10 <sup>-7</sup> ±2×10 <sup>-9</sup>
Saturation	0.8±0.2	2.9±0.2	2.3±0.2	2.9±0.8	0.45±0.02
Deep	0.0318±0.0007	0	2.46×10 <sup>-3</sup> ±2×10 <sup>-5</sup>		8.15×10 <sup>-8</sup> ±2×10 <sup>-9</sup>
Saturation	1.95±0.04	0	5.64±0.04	2.89±0.06	0.33±0.02

these calculations, as it determines the extent to which gases will be concentrated and fractionated. The scenario has implications for changes in the hydrological balance of the system that are required to produce these observations, and these implications are discussed. We stress, however, that because of the unconstrained nature of the system and the limited data at hand, definitive explanations for the observations are not presently possible.

To determine the total dissolved gas pressure for the system, it is necessary to include measurements of O<sub>2</sub> and N<sub>2</sub>. Table 3 shows concentrations of the major and noble gases in the surface and bottom waters. Nitrogen, oxygen, and argon constitute ~99% of the total dissolved gas load. The N<sub>2</sub> undersaturation at the ice-water interface could result from a combination of biological processes and interactions with the ice, but this hypothesis is not addressed herein. We assume in our calculations that N<sub>2</sub> behaves as an inert gas that is not soluble in the ice. As discussed above, He, Ne, and Ar are well predicted by the three-phase model, providing some confidence that the system is in approximate balance between the total dissolved gas pressure and the hydrostatic pressure at the ice-water interface. The hydrostatic pressure at the interface (~5 m) is ~1.45 atm. The equilibrium total dissolved gas pressure is determined by the hydrostatic pressure and the pressure required for heterogeneous bubble nucleation, which is often in slight excess of hydrostatic pressure in natural systems (Bari and Hallet 1974; Swanger and Rhines 1972). Instead, we use the observed concentrations of the major gases at the interface to determine a "stability gas load" for the system, and use this as a reference equilibrium value at the interface. The total dissolved gas concentration at the interface is ~4.52 × 10<sup>-2</sup> cc (STP) g<sup>-1</sup>. If freezing were to continue, the total gas concentration in the water would remain at or near this stability gas load, with any excess due to increased freezing being removed by further bubble formation. The only way to increase inert gas concentrations in a closed system is to remove one or more of the major gases by another mechanism, thus lowering the total dissolved gas concentration and allowing the other gases to increase until the sum of the partial pressures of the remaining gases equals the stability gas load.

Comparisons of surface- and bottom-water concentrations show a dramatic decrease in O<sub>2</sub> concentrations and a concomitant rise in concentrations of N<sub>2</sub> and Ar. One possible scenario to explain these observations begins with the assumption that at some time in the past, the ice-water interface was near the level of anoxia. Meltwater enters the lake with solubility equilibrium gas concentrations. Freezing begins, and the gases become concentrated until the critical

dissolved gas pressure for bubble formation is reached. Bubbles form, and the gases are removed and fractionated according to their partition coefficients in the same manner described for current processes. The oxygen remaining is consumed or significantly reduced, and the total dissolved gas pressure decreases to below the critical dissolved gas pressure for bubble formation. Freezing thus continues with no bubble formation, creating the large saturations of Ar and N<sub>2</sub> observed in bottom water.

The surface- and bottom-water dissolved gas concentrations can be used to support and constrain this mechanism. In the bottom water, the O<sub>2</sub> concentrations go to zero, decreasing the total dissolved gas concentration to ~3.90 × 10<sup>-2</sup> cc (STP) g<sup>-1</sup>, which is not sufficient for bubble formation. The Ar:N<sub>2</sub> ratio has the same value in both surface and bottom waters, implying that the only fractionation mechanisms are those occurring presently at the interface. By taking the surface-water concentrations of Ar and N<sub>2</sub> and calculating the amount of water that must be frozen with no bubble formation to produce the bottom-water concentrations, we find that only an additional ~10% of the original meltwater input would have had to be frozen. Clearly, generating the bottom-water saturations in this manner does not require drastic changes to the current system.

An additional constraint is the concentration of Ne in the bottom water. While Ar and N<sub>2</sub> concentrations would simply increase due to freezing with no bubble formation, Ne would still be removed from the system owing to its solubility in the ice. By using the above scenario and calculating the volume of ice formed from the additional freezing with no bubble formation, we estimate that the Ne concentration in the residual water should be ~33 ± 2% of solubility equilibrium (using the solubility values of Kahane et al. 1969), which is in excellent agreement with our observations (Table 3, Fig. 2A). By using the solubility values of Namoiit and Bukhgalter (1965), we estimate a Ne concentration of 42 ± 2% of solubility equilibrium, which is inconsistent with our observations.

While the required changes in the individual lake processes are not large, they do imply that the hydrological balance of the system has changed significantly over the history of the lake. For example, the requirement that the ice-water interface be near the level of anoxia at the time the bottom-water concentrations were generated could be met in several ways. If conditions in the dry valleys were such that the ice cover became significantly covered with snow relative to present conditions, the albedo of the area would be reduced and the meltwater entering the lake would decrease. Owing to the imbalance of water input and freez-

ing, the lake level would decrease and the ice thickness would increase. The light penetrating the ice cover would be reduced due to the increased thickness and snow cover, and the biological productivity of the lake would most likely decrease. These responses would serve to move the ice-water interface toward the level of anoxia, currently at ~9 meters. The response of lake levels to changes in climate is very complex in the dry valley areas (Chinn 1993), and the above scenario should only be viewed as an illustration of possible processes that could generate the observations.

The bathymetry of the lake also includes a pronounced shelf at the 9-m level, which may indicate the level at which the ice-water interface rested at some time. This speculation is supported by paleoclimatic theories (Wilson 1979) that the lakes experienced a near-desiccation event before reexpanding to their present size at about 1,200 years ago. The reexpansion is presumed to have happened fairly rapidly, which would create an abrupt step function in the concentrations of the dissolved gases between the homogeneous bottom waters and the new input water. This step function would, over time, diffuse into a profile resembling the observed shape of the Ar and density profiles.

Additional mechanisms are required to explain the He concentrations. Helium increases in the bottom water, rather than decreasing like Ne as the model predicts, and the observed  $^3\text{He} : ^4\text{He}$  ratios (Fig. 2B) require a nonatmospheric helium flux into the bottom of the lake. Assuming that vertical transport is limited to molecular diffusion (*see below*), we calculate a  $^4\text{He}$  flux of at least  $2.3 \pm 0.4 \times 10^8$  atoms  $\text{m}^{-2} \text{s}^{-1}$ , and a  $^3\text{He}$  flux of  $\sim 2 \times 10^2$  atoms  $\text{m}^{-2} \text{s}^{-1}$ . We calculate that the  $^4\text{He}$  flux can be supported by decay of U and Th in 230 m of lake sediments, consistent with the thickness observed in the Dry Valley Drilling Project drill holes in the area (Purucker et al. 1981). However, the  $^3\text{He} : ^4\text{He}$  ratio is  $9 \pm 1 \times 10^{-7}$ , which is much greater than a radiogenic production ratio (Andrews 1985), thus requiring an additional source for the  $^3\text{He}$ . We contend that the  $^3\text{He}$  could be supported by loss of cosmogenic  $^3\text{He}$  from the bottom sediment, which enters the lake with glacial meltwater during the summer. The cosmogenically produced  $^3\text{He}$  concentration in Dry Valley sediments is  $650 \pm 137 \times 10^6$  atoms  $\text{g}^{-1}$  (Brook and Kurz 1993). The observed flux of  $^3\text{He}$  in the lake is consistent with a loss rate from the sediments of only 3% per million years, which is smaller than the predicted loss rate of 10% per million years (Trull et al. 1991). While the Dry Valley sediments analyzed may not be representative of those at the bottom of the lake, the above calculations and the pronounced  $^3\text{He}$  gradient in the bottom water are consistent with input of  $^3\text{He}$  from the sediment.

**Ventilation rates and mechanisms**—While the relatively homogeneous vertical profile of tritium in the upper water (Fig. 3B) is suggestive of rapid vertical mixing, it is most likely the result of a temporal decrease in tritium input to the lake that is approximately equal to decay (half-life of 12.43 years). The pronounced vertical gradient in the tritium- $^3\text{He}$  age profile (Fig. 3A) is inconsistent with rapid vertical mixing and is qualitatively consistent with ventilation times of the upper lake ranging from a few years at the ice-water interface to several decades at the base of the oxic layer.

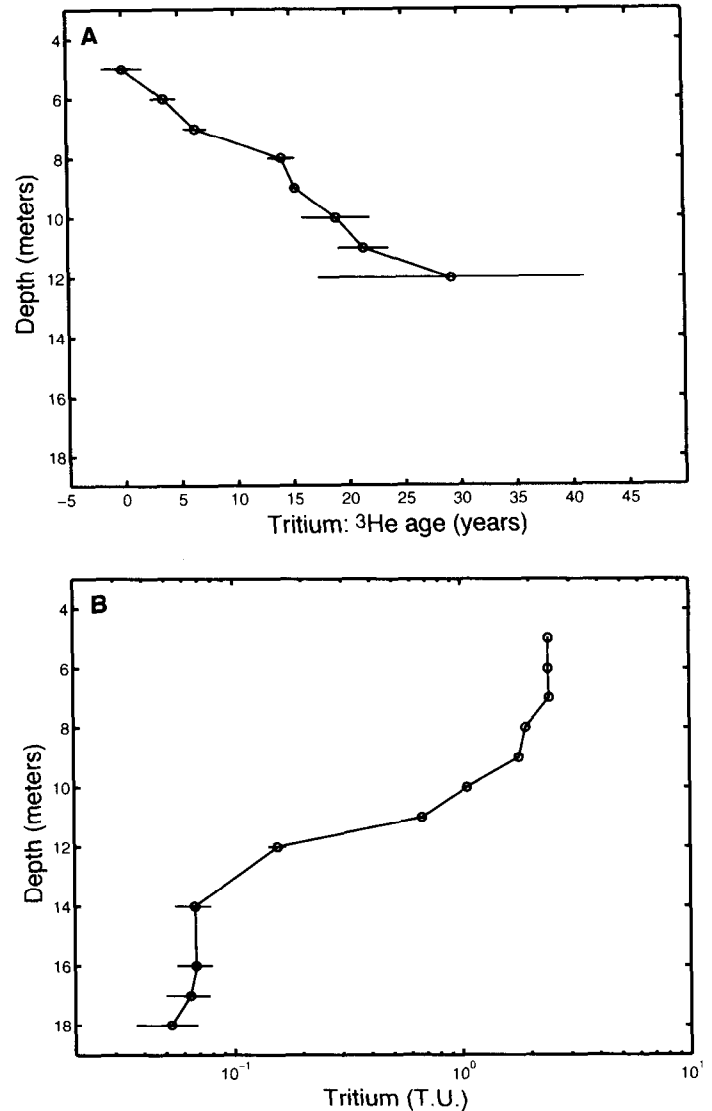


Fig. 3. A. Tritium- $^3\text{He}$  "age" equals  $17.96 \ln(\xi/\theta)$ , where  $\xi$  is the sum of the tritium and the excess  $^3\text{He}$  concentrations, and  $\theta$  is the tritium concentration. B. Tritium profile. One tritium unit (T.U.) equals  $^3\text{H}/^1\text{H} \times 10^{18}$ . The scale height of the tritium concentration gradient is calculated using  $(\kappa/\lambda)^{-1/2}$ , where  $\kappa$  is the diffusion coefficient and  $\lambda$  is the decay constant for tritium.

Below this depth, it is not meaningful to date the water using the tritium- $^3\text{He}$  age method. Green et al. (1989) estimate an age of a few thousand years for the bottom water of Lake Fryxell, based on the chloride budget for the lake. There is an abrupt change in the tritium concentration between the upper and lower layers of the lake, with a scale height of 1–2 m, consistent with vertical mixing that is not much greater than molecular diffusion.

Within the anoxic waters, the average tritium concentration is  $0.063 \pm 0.007$  T.U., more than 6 times the detection limit for the measurements and more than 25 times the potential contamination levels (Jenkins et al. 1983). This relatively homogeneous vertical profile of tritium in the bottom water requires a mechanism that delivers tritium directly to

the bottom water, yet does not disturb the diffusional gradients observed for the inert gases. This could be explained by a weak ventilation process that occurs when relatively dense water is created at shallow lake margins due to ice formation, where the residual dense water is trapped between the advancing ice front and the lake bottom and becomes concentrated as freezing progresses. The ice around the margin of the lake grounds from the lake edge inward, causing the brine to move along the basin edges and sink to a level of neutral buoyancy. Evidence of this type of haline circulation has been found in other Antarctic saline lakes (Ferris et al. 1991). To prevent significant disturbance of the gradients in the bottom water, this ventilation mechanism must be weak relative to the timescale of vertical exchange.

By reconstructing a history of tritium in the surface water of the lake, we can estimate the ventilation rate for the deep water that is required to create the current concentrations of tritium in the bottom water. The meltwater input to the lake is predominantly from glacial meltwater, with a small additional volume from snowmelt. The history of tritium in the surface water is a function of the concentration of tritium of the glacier meltwater and the history of tritium in local precipitation. We measured an average tritium concentration of  $0.104 \pm 0.02$  T.U. for the Canada Glacier, and  $2.51 \pm 0.03$  T.U. for the input (moat) water of Lake Fryxell. Precipitation in Antarctica has returned to background (pre-bomb) tritium concentrations (Jouzel et al. 1982), having an estimated value of  $\sim 23 \pm 1$  T.U. for the Dry Valleys. Using these values, we calculated an input water ratio of glacier meltwater to snow meltwater of  $\sim 10:1$ . The uncertainty in this estimate is on the order of 50%, based on variability in individual tritium measurements in precipitation from the South Pole (Jouzel et al. 1982). This variability is most likely due to seasonal variation in precipitation and deposition of tritium.

To a first approximation, the tritium concentration of the input water to the lake can be scaled to the history of tritium deposition at the South Pole by using the records of Jouzel et al. (1979) and the equation

$$C_w^{(i)} = C_g[V_g/(V_g + V_p)] + C_w^0(D_{sp}^{(i)}/D_{sp}^0), \quad (2)$$

where  $C_w$  is the concentration of tritium in the input water to the lake at time step  $i$ ,  $C_g$  is the concentration of tritium in the glacier,  $C_w^0$  is the concentration of tritium in the input water to the lake at steady-state (pre-bomb) tritium concentrations, and  $D_{sp}$  and  $D_{sp}^0$  are the deposition of tritium (in meters  $\times$  T.U./year) at the South Pole for time step  $i$  and at steady state, respectively. We linearly interpolated the record from 1977 to 1995 by using current (i.e. background) values of tritium in precipitation at the South Pole (Jouzel et al. 1982). The reconstructed history of tritium in the input water to the lake is shown in Fig. 4. Based on the fractionation of hydrogen during freezing (Weston 1955), we estimate that tritium should be enriched in the ice relative to the water by  $\sim 4\%$ . The input-water values are adjusted for this effect prior to delivery to the bottom water. Because the concentration of tritium in the glaciers is only  $\sim 4\%$  of the concentration of the input water, uncertainties in the estimate of the ratio of the volume of input water from glacial melt to the total volume of input water contributes an uncertainty to the input-water concentration of  $\sim 2\%$ . The overall uncertainty

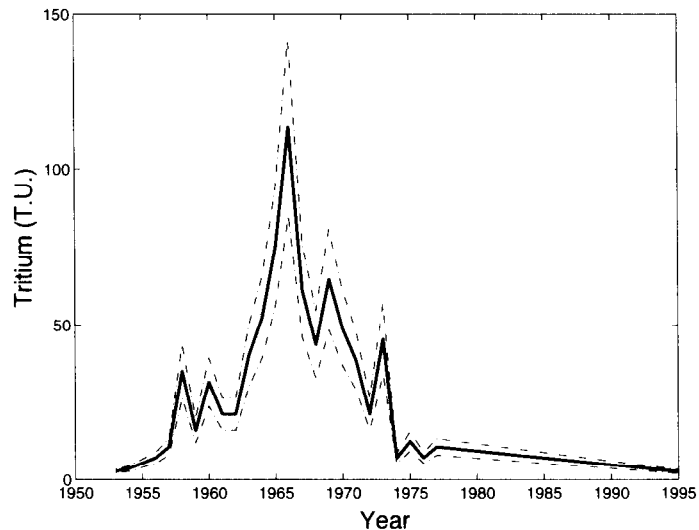


Fig. 4. Constructed tritium history for the input water. Uncertainties are shown as dashed lines.

in the estimate of the history of tritium in the input water to the lake is predominantly from the uncertainty in the measurements of the deposition of tritium at the South Pole, which is  $\sim 25\%$ .

*History of tritium in the bottom water*—The tritium record in the bottom water of the lake is a function of the surface-water concentration history, decay of tritium, and the turnover time, given by

$$\delta C_b / \delta t = 1/\tau(C_s - C_b) - \lambda C_b, \quad (3)$$

where  $C_b$  is the bottom-water concentration,  $C_s$  is the surface-water concentration corrected for fractionation effects,  $\lambda$  is the decay constant for tritium ( $0.0558 \text{ yr}^{-1}$ ), and  $\tau$  is the turnover time in years. To describe this process, we use a finite difference scheme:

$$C_b^{(i+1)} = (1 - \lambda \Delta t)C_b^{(i)} + (\Delta t/\tau)(C_s^{(i)} - C_b^{(i)}), \quad (4)$$

where the superscripts  $(i)$  and  $(i + 1)$  represent current and successive time steps, and  $\Delta t$  is 1 year. The concentration of the bottom water at steady state (pre-bomb) is given by

$$C_b^0 = C_s^0 / (1 + \lambda \tau), \quad (5)$$

where  $C_b^0$  and  $C_s^0$  are the initial steady-state concentrations, with  $C_s^0$  estimated from Eq. 5 for pre-bomb values of tritium in precipitation. The turnover time for the bottom water of the lake was determined by choosing the value of  $\tau$  that results in the best approximation of the current tritium observations of  $0.063 \pm 0.007$  T.U. The model was integrated from 1953, prior to bomb tritium reaching Antarctica, to the present in time increments of 1 year. Our calculations estimate a turnover time of 3,800 years. By running the model with the maximum and minimum possible values of surface-water tritium concentrations, we obtain a range of the turnover time from 2,600 to 5,300 years. The turnover time should not be regarded as an age of the bottom layer of the lake, but rather the renewal time associated with one mechanism of ventilation that has been operating over at least the

last 2–3 decades. Comparison of this time to age estimates of a few thousand years (Green et al. 1989) suggests that the ventilation of the bottom water may have changed considerably over time. The fact that the tritium profile in the bottom water is relatively homogeneous is a reflection of the relative, evenly distributed rates of ventilation as a function of density, rather than an indication of vertical mixing. The diffusion-length timescale associated with the development of the observed  $^3\text{He}$  gradient is  $\sim 350$  years, which is an order of magnitude faster than the estimated ventilation time, suggesting that this ventilation mechanism would not significantly disturb the dissolved gas gradients.

By using the estimate of the turnover time and an estimate of the volume of the bottom of the lake between 12 and 18 m, as taken from the bathymetry data of Lawrence and Hendy (1985), we estimated an upper limit for the yearly volume delivery to the bottom water via this ventilation process of  $\sim 5 \times 10^5$  liters. This volume must come from water remaining after freezing in the shallow margins of the lake. To estimate the original volume of water prior to freezing required by this ventilation mechanism, we used the salinity budget for the system. Green et al. (1988) reported chloride concentrations of the inflow streams of 0.271 mM, compared with concentrations at 17 m of 102 mM. The bottom-water concentration may be obtained by freezing  $\sim 99.75\%$  of a volume of water at the stream inflow concentrations. We assumed, as a first approximation, that the concentration of the residual brine in the shallow water is equal to that in the bottom of the lake, and we estimated that the volume of water required to produce the required volume of brine after freezing is  $\sim 2 \times 10^8$  liters. We estimated the volume of water shoreward of the 3-m isobath (i.e. where grounding of the ice is most likely to occur) to be  $\sim 5 \times 10^9$  liters. Thus, the proposed ventilation mechanism would require only  $\sim 4\%$  of this available volume.

Implicit in this calculation, however, is the assumption that the brine from the margins remains unmixed as it sinks to the bottom. This is clearly not a very realistic situation, and it implies that if mixing is occurring, the concentration of the brine in the margins would have to be substantially greater than that of the bottom water before sinking. Because the volume of the original water at stream-input concentrations has already been reduced by  $\sim 99.75\%$  to achieve the concentrations observed in the bottom water, a further increase in the brine concentration would most likely require multiple freezing stages, i.e. freezing water in shallow depressions of the margins that had already been concentrated by a prior freezing event. The bathymetry (Lawrence and Hendy 1985) indeed shows many shallow depressions around the periphery of the lake where such events could potentially occur, but more quantitative information about the likelihood of this mechanism is not possible with the present information. Additionally, the estimate assumes that the concentration of the brine in the bottom water is only the result of this dense water formation process in the margins of the lake and not residual brine from a prior desiccation event. With the available data and the volume constraints of the system, the proposed ventilation mechanism appears likely, but a more rigorous analysis is not possible at this time.

The consequence of this flux of water to the bottom of the lake is that there must be an upward advection of water to balance it. We calculate an upward advection of between 1 and 2 m  $\text{kyr}^{-1}$  near the top of the anoxic layer, which is not strong enough to greatly disturb the strong gradients within the lake, but which may partly explain the observed curvature in the dissolved gas profiles.

## Summary and conclusions

The lack of significant vertical mixing within Lake Fryxell provides a unique environment in which the noble gases and tritium can be used to examine the current physical processes affecting dissolved gas cycles and ventilation rates, and also to reconstruct processes that may have affected the lake over hundreds to thousands of years ago. The oxic layer is ventilated on the timescale of several decades. The linear trend of the tritium- $^3\text{He}$  age profile indicates that the water column is highly stratified, even in the upper few meters of the water column below the ice. This information, along with the three-phase equilibrium-partitioning model presented can be used to characterize the cycles of the noble gases in this system, which can provide constraints on the cycles of other dissolved gases, such as  $\text{N}_2$  and  $\text{O}_2$ , as well as provide the framework for future investigations of primary productivity in the lake.

To the best of our knowledge, the effects of the combined processes of uptake by bubbles and solubility of He and Ne in ice have never been observed on such a large scale in nature. These effects are quite dramatic here due to the unique, insulated nature of a permanently ice-covered, highly stratified lake. The undersaturations of He and Ne at the ice-water interface provide a striking contrast to the supersaturations of the heavier gases. Top et al. (1983) first recognized ice formation effects on the noble gases in natural aquatic systems, and they suggested that this anomaly may have applications as a water mass tracer. Schlosser (1986) demonstrated the potential of using supersaturations of  $^3\text{He}$  from the melting of ice as a tracer of ice-water interactions. These same processes of equilibrium distribution control the dissolved gas cycles in all aquatic systems where ice formation occurs, but the anomaly may vary between systems due to differences in the environment and ice structure.

In the bottom water, the lack of information about the system prevents more definitive conclusions, but our proposed scenario appears consistent with the available information. For a more complete treatment, it would be necessary to estimate the budgets of  $\text{O}_2$  and carbon in the lake under the proposed conditions in order to determine if a limited amount of biological productivity or a chemical sink could remove a significant portion of the  $\text{O}_2$  entering the system with fresh meltwater input. It would also be necessary to determine whether the lowering ice-water interface was from an increase in the ice thickness or from a total lowering of the entire ice-lake water system. This would have bearing on the hydrostatic pressure at the ice-water interface, which determines whether bubbles will form and fractionate the gases. In general, we suggest that the bottom-water dissolved gas concentrations are largely relict concen-

trations that resulted from a hydrological balance of the system quite different than that operating today.

### References

- BARI, S. A., AND J. HALLETT. 1974. Nucleation and growth of bubbles at an ice-water interface. *J. Glaciol.* **13**: 489-520.
- BROOK, E. J., AND M. D. KURZ. 1993. Surface exposure chronology using in situ cosmogenic  $^3\text{He}$  in Antarctic quartz sandstone boulders. *Quaternary Res.* **39**: 1-10.
- BURTON, H. R. 1981. Chemistry, physics and evolution of Antarctic saline lakes. *Hydrobiologia* **82**: 339-362.
- CARTE, A. E. 1961. Air bubbles in ice. *Proc. Phys. Soc. Lond.* **77**: 757-768.
- CHINN, T. J. 1993. Physical hydrology of the Dry Valley Lakes. *Antarct. Res. Ser.* **59**: 1-52.
- CLARKE, W. B., W. J. JENKINS, AND Z. TOP. 1976. Determination of tritium by mass-spectrometric measurement of  $^3\text{He}$ . *Int. J. Appl. Rad. Isotopes* **27**: 512-522.
- CRAIG, H., R. A. WHARTON, JR., AND C.P. MCKAY. 1992. Oxygen supersaturation in ice-covered Antarctic lakes: biological versus physical contributions. *Science* **255**: 218-221.
- FERRIS, J. M., J. A. E. GIBSON, AND H.R. BURTON. 1991. Evidence of density currents with the potential to promote micromixis in ice-covered saline lakes. *Palaeogeogr., Palaeoclimatol., Palaeoecol.* **84**: 99-107.
- GREEN, W. J., M. P. ANGLE, AND K. E. CHAVE. 1988. The geochemistry of Antarctic streams and their role in the evolution of four lakes of the McMurdo Dry Valleys. *Geochim. Cosmochim. Acta* **52**: 1265-1274.
- , T. J. GARDNER, T. G. FERDELMAN, M. P. ANGLE, L. C. VARNER, AND P. NIXON. 1989. Geochemical processes in the Lake Fryxell basin (Victoria Land, Antarctica). *Hydrobiologia* **172**: 129-148.
- JENKINS, W. J., D. E. LOTT, M. W. PRATT, AND R. D. BOUDREAU. 1983. Anthropogenic tritium in South Atlantic bottom water. *Nature* **305**: 45-46.
- JOUZEL, J. L., MERLIVAT, D., MAZAUDIER, M., POURCHET, AND C. LORUIS. 1982. Natural tritium deposition over Antarctica and estimation of the mean global production rate. *Geophys. Res. Lett.* **9**: 1191-1194.
- , ———, M. POURCHET, AND C. LORUIS. 1979. A continuous record of artificial tritium fallout at the South Pole (1954-1978). *Earth Planet. Sci. Lett.* **45**: 188-200.
- KAHANE, A., J. KLINGER, AND M. PHILIPPE. 1969. Dopage sélectif de la glace monocristalline avec de l'hélium et du néon. *Solid State Commun.* **7**: 1055-1056.
- LAWRENCE, M. J. F., AND C. H. HENDY. 1985. Water column and sediment characteristics of Lake Fryxell, Taylor Valley, Antarctica. *N. Z. J. Geol. Geophys.* **28**: 543-552.
- LOTT, D. E. AND W. J. JENKINS. 1984. An automated cryogenic charcoal trap system for helium isotope mass spectrometry. *Rev. Sci. Instrum.* **55**: 1982-1988.
- NAMOI, A., AND E. B. BUKHGALTER. 1965. Clathrates formed by gases in ice. *J. Struct. Chem.* **6**: 911-912.
- PURUCKER, M. E., D. P. ELSTON, AND S. L. BRESSLER. 1981. Magnetic stratigraphy of Late Cenozoic glaciogenic sediments from drill cores, Taylor Valley, Transantarctic Mountains, Antarctica, p. 109-129. *In* Dry Valley drilling project. Antarctic Research Series. V. 33. AGU.
- SCHLOSSER, P. 1986. Helium: A new tracer in Antarctic oceanography. *Nature* **321**: 233-235.
- SMITH, R. L., L. G. MILLER, AND B. L. HOWES. 1993. The geochemistry of methane in Lake Fryxell, an amictic, permanently ice-covered, antarctic lake. *Biochemistry* **21**: 95-115.
- SWANGER, L. A., AND W. C. RHINES. 1972. On the necessary conditions for homogeneous nucleation of gas bubbles in liquids. *J. Crystal Growth* **12**: 323-326.
- TOP, Z., W. B. CLARKE, AND R. M. MOORE. 1983. Anomalous neon-helium ratios in the Arctic Ocean. *Geophys. Res. Lett.* **10**: 1168-1171.
- TRULL, T. W., M. D. KURZ, AND W. J. JENKINS. 1991. Diffusion of cosmogenic  $^3\text{He}$  in olivine and quartz: Implications for surface exposure dating. *Earth Planet. Sci. Lett.* **103**: 241-256.
- WEISS, R. F. 1969. Piggyback sampler for dissolved gas studies on sealed water samples. *Deep-Sea Res.* **15**: 695-699.
- . 1970. The solubility of nitrogen, oxygen and argon in water and seawater. *Deep-Sea Res.* **17**: 721-735.
- . 1971. Solubility of helium and neon in water and seawater. *J. Chem. Eng. Data* **16**: 235-241.
- WESTON, R. E., JR. 1955. Hydrogen isotope fractionation between ice and water. *Geochim. Cosmochim. Acta* **8**: 281-284.
- WHARTON, R. A. JR., W. B. LYONS, AND D. J. DES MARAIS. 1993. Stable isotopic biogeochemistry of carbon and nitrogen in a perennially ice-covered Antarctic lake. *Chem. Geol. (Isotope Geosci. Sect.)* **107**: 159-172.
- , G.M. SIMMONS, JR., AND C. P. MCKAY. 1989. Perennially ice-covered Lake Hoare, Antarctica: Physical environment, biology, and sedimentation. *Hydrobiologia* **172**: 305-320.
- WILSON, A. T. 1979. Geochemical problems of the Antarctic dry areas. *Nature* **280**: 205-208.

Received: 13 July 1996

Accepted: 16 July 1997

Amended: 18 August 1997